Structural properties of amorphous hydrogenated carbon. I. A high-resolution neutron-diffraction study

J. K. Walters, P. J. R. Honeybone, D. W. Huxley, and R. J. Newport
Physics Laboratory, The University, Canterbury, Kent, CT2 7NR, United Kingdom

W. S. Howells
Neutron Division, Rutherford Appleton Laboratory, Didcot, OX11 0QX, United Kingdom
(Received 27 September 1993)

The structure of samples of amorphous hydrogenated carbon, prepared from acetylene and propane precursors, containing 35 and 32 at. % hydrogen, respectively, was investigated by time-of-flight neutron diffraction in the range 0.2–50 $Å^{-1}$ using the ISIS spallation source. The large dynamic range of the data ensures a real-space resolution sufficient to reveal directly the proportions of sp^2 and sp^3 hybridized carbon. The results show that, in these hard carbon materials, the carbon-atom sites are predominantly sp^2 bonded, and the carbon-carbon single bond:carbon-carbon double bond ratio is about 2.5:1. The detailed information on atomic correlations thus provided is used to discuss current structural models, and in particular the data are used to show that these models require significant modification.

INTRODUCTION

For a period of over two decades there has been continual growth in our knowledge of amorphous materials and our understanding of their properties, accompanied by their technological exploitation. Important questions remain unanswered concerning their properties, however—a situation exacerbated by the increasing complexity of novel materials—and amorphous materials therefore maintain their position of continued fundamental and technological interest. A prime example of this is the now extensive work on amorphous hydrogenated silicon, *a*-Si:H.[1] In fact, as novel materials continue to be generated, the range of questions only increases.

The material at the focus of our investigation here, amorphous hydrogenated carbon, *a*-C:H, is of particular interest as it may be prepared harder, denser, and more resistant to chemical attack than any other solid hydrocarbon,[2,3] which, together with the high degree of transparency to the infrared and histocompatibility, have led to many applications.[4,5] The macroscopic properties of the material are, however, critically dependent on the conditions under which it was prepared.[6] *a*-C:H can be prepared in forms varying from the soft polymeric (high hydrogen content with many $-CH_2-$chains) at one extreme and graphitic (high sp^2 content, low hydrogen content) at the other. Polymeric *a*-C:H films are deposited under conditions having intrinsically low incident particle energies, whereas the graphitic analog arises from deposition conditions in which there are high incident energies which causes preferential sputtering of hydrogen. Hard, or "diamondlike" *a*-C:H form under conditions of intermediate deposition energies, which result in a large degree of crosslinking and structural rigidity and intermediate hydrogen content.[2]

In spite of the great potential of the material and the studies so far undertaken, e.g., Refs. 6–8, the structure of these materials at the atomic level is not fully understood; this is of course largely due to the range of potential bonding environments which allows a complex mixing of atomic-scale correlations.

Current models for the structure involve aromatic/graphitic clusters of sp^2 carbon interconnected with a hydrogenated (or polymeric) sp^3 phase; a more detailed account of these models can be found in the reviews by Angus, Koidl, and Domitz[2] and Robertson.[3,6,9,10] Data presented here suggest this may be an unsuitable model for *a*-C:H, especially at higher hydrogen concentrations, where sp^2 carbon concentrations are lowest.

The suggestion is supported by the recent results of Frauenheim *et al.*[11] (and extended greatly in paper IV of this series) on molecular-dynamics simulation studies of viable structures. Their findings show a system of short chainlike segments showing a markedly low tendency towards aromaticity. The sp^2 atoms are interconnected by homogeneously distributed sp^3 chainlike segments. One must bear in mind of course the intrinsic limitations of finite box-sized (in this case 64 atoms) simulations using approximated potentials, but the molecular-dynamics results are clearly at variance with the current models.

The precise nature of the bonding in *a*-C:H obviously has a crucial role to play in determining the bulk properties, particularly the sp^2:sp^3 ratio, as these two carbon bonding environments lead to vastly different physical characteristics (e.g., diamond and graphite). Of the studies carried out hitherto the results have given sp^2:sp^3 ratios varying between 1:2 and 2:1, depending on exact deposition conditions, with optical band-gap measurements consistent with the current model of a high degree of clustering of sp^2 carbon sites which would indicate that intermediate, as well as short-range order is important. NMR (Refs. 7, 8, and 12), however, provides reliable information on this ratio and suggests that sp^2 atom concentrations will be slightly greater than that for sp^3 atoms for most *a*-C:H samples. Our NMR results (presented in paper III of this series) provide a very much

0163-1829/94/50(2)/831(8)/$06.00

more detailed picture than any published hitherto on these structural questions.

Attention should also be drawn to the important role played by the hydrogen in determining the properties of *a*-C:H; a role which is crucial to a full understanding of the material. Within the Robertson model, for instance, the hydrogen is seen to stabilize the sp^3 regions, reducing the number of network-terminating bonds, and therefore leading to a maximum hardness at intermediate hydrogen concentrations. Inelastic neutron scattering can be used to focus on the hydrogen vibration modes in *a*-C:H and can therefore act as a detailed probe for looking at the hydrogen environment; paper II in this series will present and discuss the quantitative (cf. infrared and Raman spectroscopy) data derived from such experiments.

Diffraction experiments on the other hand provide an opportunity to obtain direct information on interatomic distances and on the average numbers of atoms in each coordination shell. These have been mainly limited to x-ray[13] and electron diffraction[14] thus far; both these probes interact with the electrons surrounding the nucleus rather than the nucleus itself, and as a consequence of this light elements, especially hydrogen, are virtually invisible and are therefore not well detected by these methods. Also the range of data available in k space is intrinsically too restricted to allow the extraction of high-resolution real-space information. In particular, it is not possible to distinguish different carbon bonding environments on interatomic separations alone; only the mean separation and coordination number may be used, with the additional concern that coordination numbers are hard to determine accurately on the basis of x-ray or electron-diffraction data.

Neutron diffraction, especially from a pulsed source, overcomes this problem by allowing a significantly wider dynamic range, and with its reliance on scattering from nuclear centers rather than electron distributions, enables the hydrogen bonding environment of *a*-C:H to be studied. Moreover, the interference function (or structure factor) derived from a neutron-diffraction experiment may be placed on an absolute scale: the data are fully quantitative.

We present here data of superior real-space resolution to that available hitherto and use the information derived from it to discuss the validity of current models for the structure of *a*-C:H. Initial findings relating to two different forms of *a*-C:H have been published;[15,16] we here aim to present a full analysis of the data and to provide a consolidated and coherent discussion of the implications of these results. In paper II of this series we present complementary results (on the same samples) from an inelastic neutron-scattering study which highlights the hydrogen binding environment still further and this is suggestive of the overall nature of the network structure. Paper III adds significant additional information derived from an exhaustive series of magic angle spinning (MAS)/NMR measurements, may of which required the use of sophisticated resonance methods. The structural model suggested in paper III, derived from a synthesis of the neutron and NMR data, is itself illuminated further by comparison with the molecular-dynamics (MD) simulation results presented in paper IV.

EXPERIMENTAL DETAILS

Two samples of *a*-C:H were prepared using a saddle-field fast-atom (i.e., neutral particle) source[17,18] from acetylene and propane precursor gases, respectively. The samples were prepared at an effective beam energy of ~ 500 V (this figure differs from that given in our preliminary papers on these samples: this is due to a miscalibration of the equipment by the manufacturers, now rectified) and a system pressure of 1.4×10^{-4} mbar, and are in the form of powders derived from original thin-film deposits. These deposition conditions pertain to the hard forms of the *a*-C:H family: Knoop hardnesses of $2000H_k$ have been measured[19] for these materials (cf. $6000-11\,000H_k$ for diamond[2]), although hardnesses greater than $6000\ H_k$ have also been observed in the same series of studies. Sample densities were determined using a residual volume technique. This measured bulk density is likely to be less than the microscopic density due to the presence of voids. The compositions were obtained from Carlo-Erba CHN combustion analyses. Results of these measurements are given in Table I.

The data presented here were collected using the LAD diffractometer at the ISIS pulsed neutron facility at the Rutherford Appleton Laboratory (UK) (Ref. 20) has a wide dynamic range available ($\sim 0.2-50$ Å^{-1}). A spallation source such as ISIS produces neutrons with a spread of velocities, and therefore a spread of arrival times at any detector. This gives a smooth variation in neutron wavelength as a function of time-of-flight (tof). Neutrons are scattered from the sample into fixed angle detectors on each side of the instrument, and for each detector pair (i.e., at a given angle 2θ) the scattered intensity can be measured as a function of tof, which can be directly related to momentum transfer. The complete scattering profile is then obtained by combining overlapping spectra from several detector angles. Tof spectra are also recorded by monitors in the incident and transmitted beam to provide information on the total neutron cross section and the shape of the incident beam's intensity: wavelength profile. For each experiment, at least four mea-

TABLE I. Compositional information on the two samples.

	Precursor gas	C:H ratio in gas	C in film (at. %)	H in film (at. %)	Density (g cm^{-3})	Number density (atoms Å^{-3})
Sample 1	Acetylene	1:1	65	35	1.8	0.134
Sample 2	Propane	1:4	68	32	2.0	0.140

surements are required: the sample, the empty sample container, a background in the absence of sample, and a vanadium rod having a geometry which is comparable to the sample and its container. The vanadium rod measurement supplies the information necessary to put the sample scattering on an absolute scale since its neutron cross section is almost entirely incoherent, and is well known.[21] Figure 1 shows a schematic representation of the experimental arrangement.

In performing a diffraction experiment, the quantity we wish to obtain is the structure factor $S(Q)$, where, for an amorphous material (i.e., an isotropic scatterer):[21]

$$S(Q)=1+\frac{4\pi\rho}{Q}\int_0^\infty r\,dr[g(r)-1]\sin(Qr)\ , \qquad (1)$$

where ρ is the average number density of atoms in the material, $|\mathbf{Q}|=|\mathbf{k}_i-\mathbf{k}_f|$ is the wave-vector transfer associated with the diffraction experiment—which for scattering from a liquid or amorphous solid is defined as $Q=(4\pi/\lambda)\sin\theta$, where 2θ is the scattering angle and λ is the neutron wavelength—and $g(r)$ is the pair-correlation function, which is a measure of the atomic density at a distance r from a given atom at the origin. The pair-correlation function may be obtained by Fourier transformation of the structure factor, which is directly related to the measured neutron-scattering intensity.

In a multicomponent system there are contributions to the total structure factor from each atom-type pair. For a binary system such as a-C:H, we therefore have three terms which are weighted to give the total structure factor $F(Q)$, such that

$$F(Q)=\sum_\alpha c_\alpha^2 b_\alpha^2+\sum_{\alpha\beta} c_\alpha b_\alpha c_\beta b_\beta[S_{\alpha\beta}(Q)-1]\ , \qquad (2)$$

where c_α and c_β are the atomic fractions, and b_α and b_β are the neutron coherent scattering lengths, respectively, of elements α and β, and $S_{\alpha\beta}(Q)$ is the partial structure factor. The first summation represents the "self-" or "single-atom" scattering, while the second corresponds to the "interference" or "distinct" scattering and contains the basic information on atomic correlations. The derivation of these equations is predicated on the validity of the static approximation,[22,23] which requires that any change in a neutron's energy upon scattering is small compared to its incident energy. Fourier transformation leads to the total pair-distribution function $G(r)$:

$$G(r)=\sum_{\alpha\beta}[c_\alpha c_\beta b_\alpha b_\beta g_{\alpha\beta}(r)]\ , \qquad (3)$$

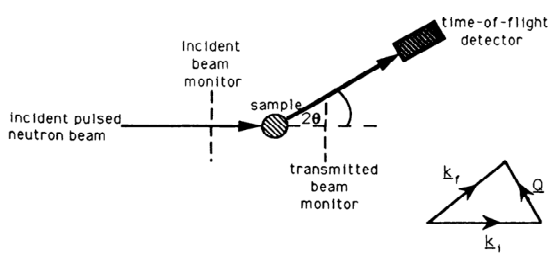

FIG. 1. A schematic representation of the experimental arrangement.

TABLE II. Normalized weighting coefficients for the partial structure factors and pair-correlation functions [see Eqs. (2) and (3)]. Units for b are fm, $c_C+c_H=1$.

	C-C	C-H	H-H
Sample 1	1.27	−0.38	0.11
Sample 2	1.85	−0.98	0.13

where $g_{\alpha\beta}(r)$ represent the partial terms in $G(r)$. From the weightings for the individual terms in the structure factor and the pair-distribution function given in Table II, it can be seen that the dominant terms will be those arising from the carbon-carbon and carbon-hydrogen correlations. (Note that the carbon-hydrogen term is negative due to the π phase shift experienced by a neutron on scattering from hydrogen; it must also be equivalent to the hydrogen-carbon correlation term.)

DATA ANALYSIS

Before obtaining the $F(Q)$ several corrections need to be applied to the data, the major ones being for background, container, and multiple scattering, attenuation and the effects of inelasticity. Full details of these may be found elsewhere.[21,24] For hydrogenous materials the inelastic scattering correction (i.e., the method by which account is taken of the deviation from purely elastic scattering, or the static approximation) is the most problematic step in the analysis procedure. The simplistic approaches to the problem[25] break down for low atomic mass systems, and alternative routes need to be found.

The high incoherent scattering cross section of hydrogen generates a large amount of self-scattering, which will change the overall level of the measured total scattering without affecting the interference function. So, isolation of the interference function is possible to a good approximation if the overall shape of the self-scattering is found. The method adopted here is an empirical method which involves fitting a low-order polynomial to the underlying curve, which is then removed from the spectra. Since the major impact of the inelasticity correction is in the self-scattering term, the subtraction of this smooth curve provides a reasonable approximation (bearing in mind the fact that current pseudoanalytic approaches to this problem[26–28] do not cope well with low-mass nuclei). The method works well for the data at $Q>\sim 2$ Å^{-1}, however, for the region below $Q\sim 2$ Å^{-1} it is less robust and as a consequence the form of the structure factor in this region is not as quantitatively reliable and this may lead to certain problems in the Fourier transformation to the pair-distribution function. In other studies of this problem[26] the interatomic distance for nitrogen, for example, is found to be 3% too short, and for deuterium the shift in Q produces a 180° phase shift in the oscillations in $\sin(Qr)$. We therefore expect the bond distances and peak areas for correlations involving hydrogen to be approximate only. Inelastic neutron scattering, however, has been used to obtain a reliable value for the H-H molecular bond length in a-C:H.[29]

RESULTS AND DISCUSSION

Figures 2 and 3 show the $F(Q)$ and $G(r)$, respectively, for samples 1 and 2. These may be compared to the neutron-diffraction data of Gaskell *et al.*[30] on mass-selected, ion-beam (MSIB) produced "amorphous diamond:" their small sample having a very low hydrogen content. That the correlation functions differ significantly in detail is of little surprise given the very different deposition conditions, hydrogen content, etc., and there is little point in attempting a detailed comparison.

The LAD diffractometer is particularly well-suited for the study of covalently bonded amorphous materials, and the exceptional real-space resolution of this data allows us to look in detail at the carbon bonding environments within the random network. Indeed, the principal point to make at this stage is that the carbon-carbon point-shell peak has a distinct shoulder on the low r side: it is therefore possible to separate out the relative contributions of the double and single bonds in the network structure in a quantitative and direct way. From the pair-distribution function $G(r)$, we obtain the radial distribution function, $J(r)$, where $J(r)=4\pi r^2\rho G(r)$, which is a measure of the number of atoms at a given radial distance, and which can then be fitted with a series of Gaussians (see Fig. 4), allowing position and area to float. By this method, accurate values for the bond lengths and coordination numbers have been obtained and these are given in Tables III and IV for the two samples. Also, for comparison, some of the known bond lengths for carbon and hydrogen are given in Table V.

Now, with such high-resolution data it is possible to go further than the straightforward assignments given in the tables. There is a clear indication that molecular hydrogen is present in both samples in relatively small quantities and this has been confirmed by inelastic neutron-scattering experiments.[29] Also the carbon-carbon bond length in both cases is slightly less than that associated with saturated carbon-carbon in diamond, which is consistent with the proximity of sp^2 carbon atoms to the single bond. Again in both samples, an unsaturated carbon-carbon bond length of 1.34 Å is observed which, because of its exact correspondence with the bond length associated with olefinic carbon, would indicate that most of the sp^2 carbon present is the olefinic and not the aromatic/graphitic form. The residuals shown in Fig. 5 show that the fits obtained using peaks at the bond distance associated with olefinic sp^2 carbon-carbon bonds, ~ 1.34 Å, are better than those obtained when a peak at ~ 1.42 Å, corresponding to graphitic/aromatic sp^2 carbon-carbon bonding is used.

More information can be gained from the Gaussian fitting process concerning the proportions of sp^3 and sp^2 carbon-atom types. Assuming all the carbon atoms are in either sp^3 or sp^2 hybridized states allows us to describe the mix of atom sites in the following form:

$$\{sp^3\}+\{sp^2\}+\{h\}=1 \ , \tag{4}$$

where $\{sp^3\}$, $\{sp^2\}$, and $\{h\}$ are the atom fractions of sp^3 hybridized carbon, sp^2 hybridized carbon, and hydrogen, respectively. If $r+1$ is the number of unsaturated bonds per sp^2 hybridized carbon atom (i.e., $r=0$ for olefinic, $r=1$ for aromatic, and $r=2$ for graphitic carbon atoms), it is possible to obtain a ratio of saturated to unsaturated carbon bonds, which is the same as the ratio of the ~ 1.34 Å:$\sim 1.52/3$ Å peak areas:

$$\frac{\text{area of } \sim 1.34 \text{ Å peak}}{\text{area of } \sim 1.52 \text{ Å peak}} = \frac{\text{unsaturated bonds}}{\text{saturated bonds}} = \frac{(1+r)\{sp^3\}}{4\{sp^3\}+(2-r)\{sp^2\}-\{h\}} \ . \tag{5}$$

However, in this case where we may assume that, to a very good approximation all the sp^2 carbon-atom types

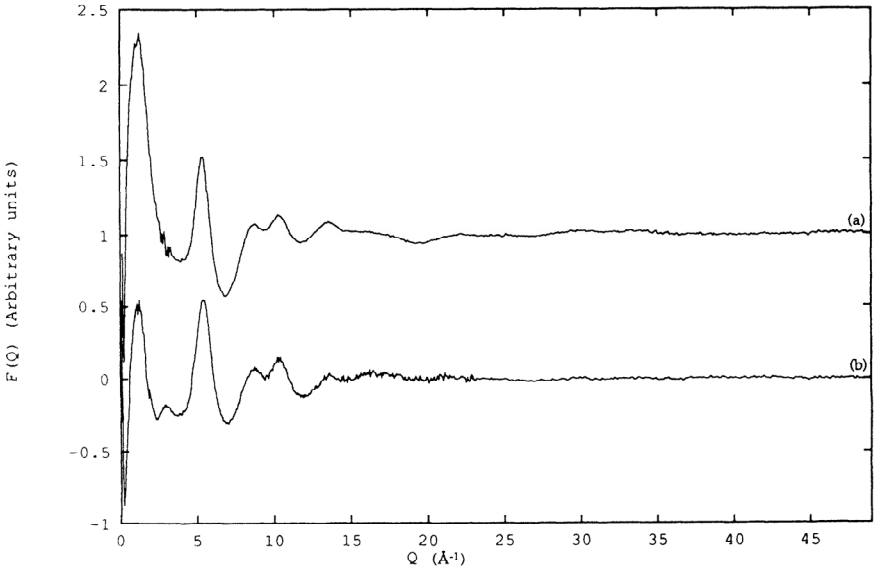

FIG. 2. The structure factors for sample 1 (a) and sample 2 (b).

TABLE III. Bond lengths and coordination numbers for Sample 1 derived from the neutron data.

Peak position (±0.01 Å)	Peak area (±0.3 atoms)	Assignment
0.88	0.84	H-H
1.03	0.18	C-H and H-C
1.34	0.84	C=C
1.52	2.17	C-C
1.7–2.2		H-C-H and C-C-H
~2.5		C-C-C

TABLE IV. Bond lengths and coordination numbers for Sample 2 derived from the neutron data.

Peak position (±0.01 Å)	Peak area (±0.3 atoms)	Assignment
0.86	0.41	H-H
1.06	0.16	C-H and H-C
1.34	1.12	C=C
1.53	2.64	C-C
1.7–2.2		H-C-H and C-C-H
~2.5		C-C-C

are in an olefinic environment, we simply put $r=0$ in Eq. (5) and together with Eq. (4) the values of $\{sp^3\}$ and $\{sp^2\}$ can be readily determined. It is therefore also possible to calculate the ratio of carbon-carbon single to double bonds. The results of these two calculations for both samples are shown in Table VI. This computation relies, of course, on our curve fitting to the $J(r)$ and, whilst peak positions may be determined with a high degree of accuracy (±0.01 Å), the associated areas have rather lower reliabilities. Given the level of the uncertainty involved (estimated by examining the effect of varying the Gaussian fit parameters, and noting that they are all correlated) it is possible that the carbon-carbon single:double bond ratio could be as high as 3.7:1. Note that although it is not possible to rule out completely contributions from aromatic or (rather less likely) graphitic carbon environments on the basis of this data, it is evident that they can only be present in very low concentrations, which is in agreement with our MNR data (paper III) and with the molecular-dynamics simulation work (paper IV). We therefore see no evidence at all for the existence of the relatively large graphitic or aromatic sp^2 clusters which form the basis of the most commonly used of the current structural models: indeed the data presented here imply that such models ought to be radically updated, at least for the family of *a*-C:H materials exemplified by the samples discussed here.

There are, however, two aspects of the data which require some comment. There is a general problem faced in the interpretation of any pair-distribution function associated with a system as structurally complex as *a*-C:H which arises from the interplay between features which are close to one another in r space. The very high real-space resolution achieved in this study has alleviated the problem to a significant degree, but the overlap between the (negative) carbon-hydrogen feature at ~1 Å and the first carbon-carbon shell correlations at ~1.5 Å remain somewhat problematic. The situation is exacerbated by the fact that residual inaccuracies in our empirical approximation to the inelasticity correction (which are of primary concern at $Q<\sim 2$ Å^{-1}) mean that as a consequence the amplitudes of features in the $G(r)$ become less reliable at the lowest r values ($<\sim 1$ Å). Hence, whilst it is evident that the (negative) first-shell carbon-hydrogen contribution to the $G(r)$ must be significant, the combined effect of the overlap with the first-shell carbon-carbon correlations and the weakly determined molecular hydrogen feature means that the C-H feature's amplitude may be somewhat suspect. There is also a possibility that there may be a small proportion of *sp* bonds (~1.2 Å)

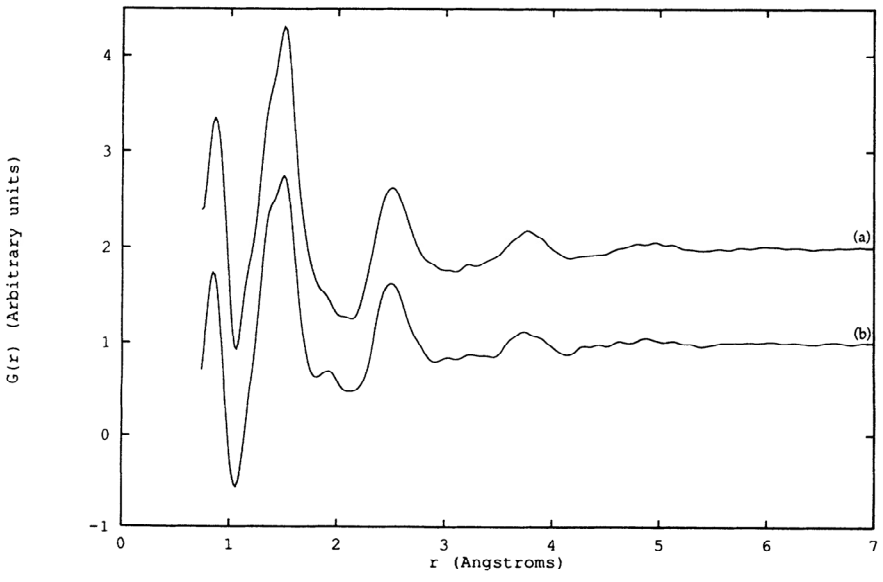

FIG. 3. The total pair-distribution functions for sample 1 (a) and sample 2 (b).

TABLE V. Bond lengths and atomic distances of carbon and hydrogen.

sp^3	C-C	Diamond	1.54 Å
sp^2	C-C	Graphite	1.42 Å
sp^2	C-C	Benzene	1.3954 Å
sp^2	C-C	Ethene	1.34 Å
sp^3	C-H	Methane	1.09 Å
sp^2	C-H	Ethene	1.07 Å
	H-H	Hydrogen	0.75 Å
sp^3	H-C-H		1.80 Å
sp^2	H-C-H		1.90 Å
sp^2	C-C-H		1.95 Å
sp^3	C-C-H		2.16 Å

present (see paper IV): these have been observed as weak features in infrared work on our samples to be published. This has, however, no material impact on our conclusions.

We are also able to provide qualitative statements concerning the nature of the correlations beyond the first coordination shells. For both samples, there is a small peak at 1.9 Å which requires some explanation. This is possibly the result of a convolution of the large carbon-carbon second-shell neighbor peak at ~2.5 Å with a "negative feature" at 2.16 Å due to an sp^3 carbon-carbon-hydrogen second-shell correlation; it is more likely however that it arises from an sp^3 or sp^2 hydrogen-carbon-hydrogen second-shell correlation (which would be expected at ~1.8–1.9 Å). Indeed, if short chains of sp^3 CH_2 exist as suggested by our NMR data (paper III),

TABLE VI. Carbon bonding environments for *a*-C:H determined by neutron diffraction.

	$\{sp^3\}$ (saturated)	$\{sp^2\}$ (unsaturated)	C-C:C=C ratio
Sample 1	0.16	0.49	2.6:1
Sample 2	0.13	0.55	2.4:1

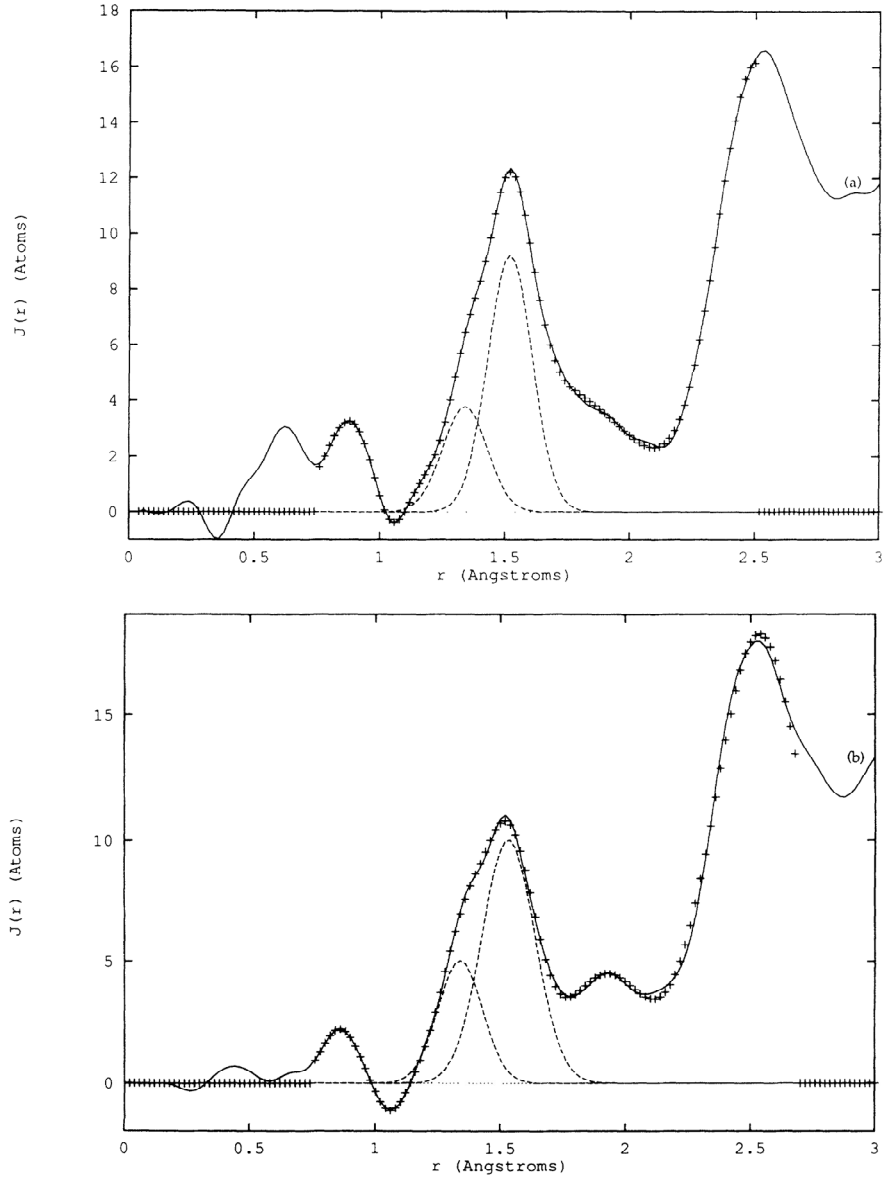

FIG. 4. The total peak fits (+) to the experimentally derived radial distribution function for sample 1 (a) and sample 2 (b), showing Gaussian components for the carbon-carbon peaks (— — —).

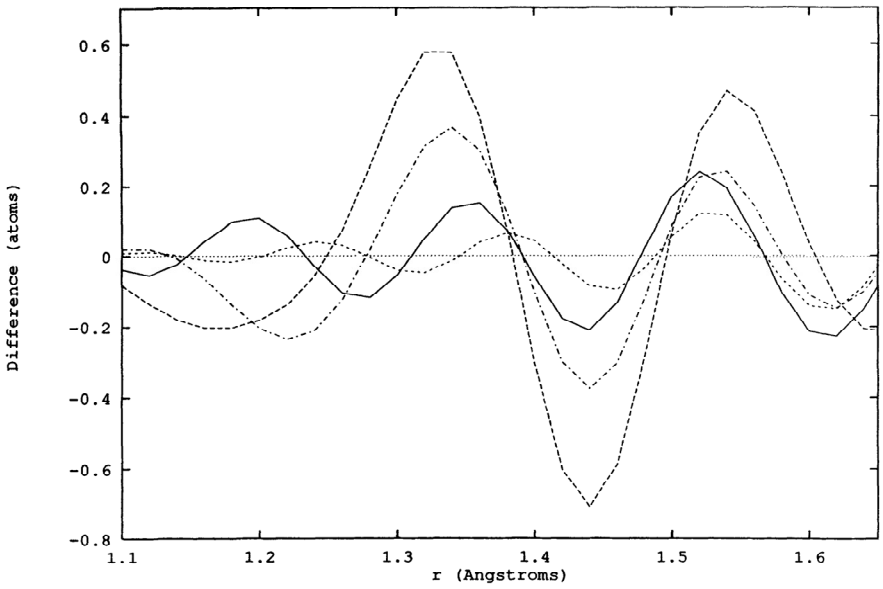

FIG. 5. The differences between observed and fitted $J(r)$ data: sample 1 (· · · ·) and sample 2 (——) using peaks at ~1.35 and ~1.53 Å, and sample 1 (— — —) and sample 2 (—·—·—·) using peaks at ~1.42 and ~1.53 Å.

then an associated H-C-H correlation may also appear at higher r values and (wholly or partially) cancel any negative-going C-C-H feature. Further experiments using H/D isotopic substitution will yield much clearer information on these questions (this work is now under way and will be reported in due course) as does our NMR data.

Using the carbon-carbon second-shell peak centered at 2.5 Å, it has been possible to generate a carbon bond angle distribution which shows a principle peak centered on the tetrahedral angle, but extending towards 120°; precise statements cannot be made because the broad 2.5-Å peak has contributions from several carbon-carbon-carbon correlations.

We can return to a qualitative comparison of these results with those for the MSIB form of amorphous carbon.[31] Their sample, with its high sp^3 carbon content shows a single first-shell peak very close to the diamond distance, albeit somewhat broader. Gaskell *et al.* do, however, note a slight inconsistency in first- and second-shell coordination numbers and propose a "new" form of carbon, intermediate between sp^2 and sp^3.[30] However, the work assumes that all sp^2 carbon is in a graphitic environment; our results, although on rather different samples, would seem to suggest that this may be a poor approximation for low sp^2 concentrations. Their discrepancy between the first- and second-shell coordination numbers is reduced without the need to invoke this "new" form of carbon if the sp^2 carbon is assumed to be all olefinic. Also we have not yet found a satisfactory method for obtaining accurate second-shell coordination numbers, since the second-shell peak has a number of contributory carbon-carbon-carbon correlations.

Although the carbon-carbon peak areas and the single:double bond ratios are the same for the two samples, within the experimental error, there are differences between them which, to some extent, indicate the effects of changing the precursor gas. Fourier transformation of the low-Q data, for instance, shows that there is weak medium-range ordering in both samples, although the degree of order is higher for sample 1 (acetylene precursor) than for sample 2 (propane precursor). From Fig. 3 it can be seen that the feature associated with the C=C bonds is more pronounced for sample 2 than for sample 1. Also, thehigher hydrogen content of the precursor gas for sample 1 compared to that from which sample 2 was prepared, is reflected in the area of the H-H peaks (see Tables III and IV). However, before any detailed conclusions can be drawn from neutron-diffraction data, the effect of the precursor gas needs further investigation with an increased variety of gases and/or the use of H_2 dilution. NMR work on these samples (see paper III does pick up quite clear differences between them also, and it is suggested that at least some of the residual differences between experiment and MD simulation arise from the analogous fact that the starting configuration in the MD work comprises separate carbon and hydrogen atoms at low density and high temperature. This latter point is the subject of further discussion in paper IV. Also, small-angle x-ray-scattering measurements are already underway to investigate the presence of voids.

CONCLUSION

The high real-space resolution results presented here show that the carbon sites in hard a-C:H are predominantly sp^2 hybridized, even in intermediate hydrogen content samples. The single:double bond ratio is shown to be ~2.5:1. Furthermore, the unsaturated C=C bond distance of 1.34 Å is too short to be aromatic or graphitic in character and corresponds very closely to the olefinic bond distance. This implies that current models for the structure of a-C:H, which rely on large aromatic carbon clusters, need revision. Additional data, based on the use of H/D isotopic substitution, are required before a more detailed study, at the partial correlation function level, will be possible.

ACKNOWLEDGMENTS

We would like to thank Dr. J. Franks and Dr. P. Revell of Ion Tech. Ltd. (U.K.) for their help in depositing the samples, A. Fassam (Chemistry Dept., UKC) for his help in determining their composition. We are grateful to Dr. Th. Frauenheim and Dr. P. Blaudeck for providing us with an unpublished copy of a paper describing their molecular-dynamics studies. PJRH and JKW acknowledge the SERC for support.

[1]S. R. Elliot, Adv. Phys. **38**, 1 (1989).

[2]J. C. Angus, P. Koidl, and S. Domitz, in *Plasma Deposited Thin Films,* edited by J. Mort and F. Jansen (CRC, Boca Raton, 1986).

[3]J. Robertson, Adv. Phys. **35**, 317 (1986).

[4]A. H. Lettington, in *Diamond and Diamond-like Films and Coatings,* edited by R. E. Clausing, L. L. Horton, J. C. Angus, and P. Koidl (Plenum, New York, 1991).

[5]S. Aisenberg and F. M. Kimock, Mater. Sci. Forum, **52-53**, 1 (1989).

[6]J. Robertson, Prog. Solid State Chem. **21**, 199 (1991).

[7]M. A. Petrich, Mater. Sci. Forum **52**, 377 (1989).

[8]H. Ehrhardt, R. Kleber, A. Kruger, W. Dworschak, K. Jung, T. Muhling, F. Engelke, and M. Metz, Diamond Related Mater. **1**, 316 (1992).

[9]J. Robertson, Diamond Related Mater. **1**, 397 (1992).

[10]J. Robertson, Phys. Rev. Lett. **68**, 220 (1992).

[11]T. Frauenheim, P. Blaudeck, U. Stephan, and G. Jungnickel, Solid State Commun. **85**, 997 (1993).

[12]F. Jansen, M. Machonkin, S. Kaplan, and S. Hark, J. Vac. Sci. Technol. A **3**, 605 (1985).

[13]J. Fink, T. Muller-Heinzerling, J. Pfluger, A. Bubenzer, P. Koidl, and G. Crecelius, Solid State Commun. **47**, 887 (1983).

[14]D. R. McKenzie, L. C. Botten, and R. C. McPhedran, Phys. Rev. Lett. **51**, 280 (1983).

[15]J. K. Walters, P. J. R. Honeybone, R. J. Newport, and W. S. Howells, J. Phys. Condens. Matter **5**, L387 (1993).

[16]D. W. Huxley, P. J. R. Honeybone, R. J. Newport, W. S. Howells, and J. Franks, in *Novel Forms of Carbon,* edited by C. N. Renschler, J. J. Pouch, and D. M. Cox, MRS Symposia Proceedings No. 270 (Materials Research Society, Pittsburgh, 1992), p. 493.

[17]J. Franks, J. Vac. Sci. Technol. A **7**, 2307 (1989).

[18]J. Franks, Vacuum **34**, 259 (1984).

[19]A. Dehbi-Alaoui, A. Matthews, and J. Franks, Surf. Coat. Technol. **47**, 722 (1991).

[20]*ISIS Experimental Facilities,* edited by B. Boland and S. Whapham (Rutherfored Appleton Laboratory, 1992).

[21]R. J. Newport, in *Neutron Scattering at a Pulsed Source,* edited by R. J. Newport, B. D. Rainford, and R. Cywinski (Hilger, Bristol, 1988), p. 233.

[22]G. L. Squires, *Introduction to the Theory of Thermal Neutron Scattering* (Cambridge University Press, Cambridge, England, 1978).

[23]J. M. F. Gunn, in *Neutron Scattering at a Pulsed Source* (Ref. 21), p. 5.

[24]A. K. Soper, W. S. Howells, and A. C. Hannon (unpublished).

[25]G. Placzek, Phys. Rev. **86**, 377 (1952).

[26]J. G. Powles, Mol. Phys. **36**, 623 (1979).

[27]M. A. Howe, R. L. McGreevy, and W. S. Howells, J. Phys. Condens. Matter **1**, 3433 (1989).

[28]W. S. Howells, Nucl. Instrum. Methods Phys. Res. Sect. B **223**, 141 (1984).

[29]P. J. R. Honeybone, R. J. Newport, W. S. Howells, J. Tomkinson, S. B. Bennington, and P. J. Revell, Chem. Phys. Lett. **180**, 145 (1991).

[30]P. H. Gaskell, A. Saeed, P. Chieux, and D. R. McKenzie, Philos. Mag. B **66**, 155 (1992).

[31]P. H. Gaskell, A. Saeed, P. Chieux, and D. R. McKenzie, Phys. Rev. Lett. **67**, 1286 (1991).